Available online at www.sciencedirect.com
ScienceDirect
Polymer 47 (2006) 7653–7663
polymer
www.elsevier.com/locate/polymer

Atom transfer radical polymerized MR fluids

B. Hu [a], A. Fuchs [a,*], S. Huseyin [b], F. Gordaninejad [b], C. Evrensel [b]

[a] University of Nevada, Reno, Department of Chemical Engineering, 1664 N. Virginia St, Reno NV 89501, USA
[b] University of Nevada, Reno, Department of Mechanical Engineering, 1664 N. Virginia St, Reno NV 89501, USA

Received 11 November 2005; received in revised form 30 August 2006; accepted 31 August 2006
Available online 26 September 2006

Abstract

A novel magnetorheological fluid, in which the surface of iron particles is coated with poly(butyl acrylate) by surface-initiated atom transfer radical polymerization (ATRP), is investigated. The polymer coating procedure includes two steps, which are immobilization of initiator: 2-(4-chlorosulfonylphenyl)-ethyltrichlorosilane (CTCS) on the iron particles' surface and graft polymerization of butyl acrylate from the surface. The surface coating is characterized by FTIR and SEM. This magnetorheological fluid has controllable off-state viscosity and high shear yield stress. Coating polymer on the iron particles' surface by ATRP can significantly reduce iron particles' settling and improve stability of the MR fluid. Glass transition temperature is obtained using the step-scan DSC method. The molecular weight and conversion can be controlled by the molar ratio of monomer to initiator, reaction temperature and time. The reaction is first order determined by the plot of $\ln[M]_0/[M]$ against polymerization time.

Keywords: Atom transfer radical polymerization; Magnetorheological fluid; Kinetics

1. Introduction

Magnetorheological (MR) fluids are suspensions of magnetizable particles (e.g., iron particles) in a viscous or viscoelastic carrier fluid. They are field-controllable materials, whose rheological properties can be dramatically altered by applying a magnetic field. An MR fluid is in a free-flowing liquid state in the absence of a magnetic field. However, apparent viscosity can be increased by one or two orders of magnitude under a strong magnetic field in a very short time (milliseconds) and it exhibits solid-like characteristics [1]. The rheological behavior of MR fluids is typically described by the Bingham equation. A material with a yield stress in a magnetic field does not flow unless the applied stress exceeds the yield stress. This behavior is caused by the polarization induced in the suspended magnetic particles by the application of an external field. The interaction between the resulting induced dipoles causes the particles to form columnar structure, parallel to the applied field. These chain-like structures restrict the motion of the fluid, thereby increasing the viscous behavior and causing the yield stress in the MR fluid. The change in viscosity is continuous and reversible, for example, after removing the magnetic field the MR fluid can revert to a free-flowing liquid.

A typical MR fluid contains 20–40% by volume of pure iron particles with nearly spherical shape in a non-magnetic carrier fluid. Iron particle sizes typically range from 10^{-7} to 10^{-5} m [2]. The density of the particles is 7–8 g/cm^3. The second component of an MR fluid is the carrier fluid, which serves as a continuous insulating medium. Carrier fluids are chosen based on their rheological properties and their temperature stability. Typically mineral oils, synthetic oils, water, polyethylene glycols, silicones and other fluids are used. MR fluids often contain additives to provide lubricating properties.

One of the most significant challenges in many applications is that iron particles are very dense and easily settle. One method for overcoming the problem is to disperse the particles

* Corresponding author. Tel.: +1 775 3272227; fax: +1 775 784 4764.
E-mail address: afuchs@unr.edu (A. Fuchs).

0032-3861/$ - see front matter © 2006 Published by Elsevier Ltd.
doi:10.1016/j.polymer.2006.08.069

in a fluid exhibiting a yield stress rather than in a Newtonian fluid. Some surfactant systems and greases are potential candidates. Another possibility is to add nano-sized particles, such as fumed silica and organic clay, which can form a space particulate network [3]. Both approaches can be used to prevent sedimentation. However, they significantly increase the off-state (no magnetic field) fluid viscosity and make them unusable in some applications.

Particle coating is another approach to improve the stability of particle containing fluids. By coating the particles one may stabilize the materials to prevent undesirable interactions with the environment, or alter optical, magnetic, conductive, adsorptive, dispersive, or surface properties of the dispersed particles. Methods in which fine particles are covered with polymers may involve either interaction of a preformed polymer with the inorganic cores, or direct polymerization of monomers adsorbed on the particles' surfaces. Using the latter method, a new generation of MRFs, known as magnetorheological polymer gels (MRPGs) used in vibration control and damping devices, has been developed by Fuchs and coworkers [4–6]. These fluids contain partially crosslinked polymer gels, which are synthesized using non-stoichiometric amounts of monomers. Two MRPGs have been developed [6], one is hydrocarbon polyol polyurethane MRPG, the other is silicone MRPG. By adjusting the ratio of resin to crosslinker and percentage of diluents the off-state rheology and the sedimentation behavior of the system can be controlled. These fluids have the advantage of controllable off-state viscosity as well as reducing the settling rate of the magnetic particles in the fluid. This behavior is possible because the polymer gel distributes itself in the carrier fluid and physically adsorbs on the surface of magnetic particles, thus, preventing iron particles from approaching each other. Polymerization may take place before or after adding the magnetic particles. The latter case may result in precipitation of polymeric gel on the surface of the iron particles and improve the stability of the system [4]. However, a consideration relating to MRPG is that the interaction between polymer and iron particles' surfaces is physical absorption. Therefore the effect of inhibition of particles' sedimentation and suspension stability has been limited.

There are several other approaches to prepare inorganic particles coated with polymers: grafting of polymers onto inorganic particles treated with silane coupling agents [7,8], surface-initiated ring-opening metathesis polymerization (ROMP) on particles [9,10], self-assembled monolayer (SAM) adsorbed on particles [11,12] and graphitic coating on particles.

A novel magnetorheological fluid, which is different from the previous generation of MRPGs, was investigated. In this system, to reduce sedimentation and agglomeration, the iron particle surface is covalently grafted with poly(butyl acrylate) via surface-initiated atom transfer radical polymerization (ATRP). Grafting does not only improve the stability of the iron particles in suspension but also increases the compatibility of the particles with the carrier fluid system. The grafting polymer may reduce the net density of the iron particles so that it will lower sedimentation rate. Recently, controlled radical polymerization (CRP) has been successfully applied to surface-initiated graft polymerization in order to prepare a dense polymer layer with controlled structure on the surface of an inorganic substrate [13]. For the grafting process, the CRP technique is optimal, because this method affords control over the molecular weight, molecular weight distribution and structure of the resulting polymer. A major difference between conventional radical and controlled radical polymerizations is the lifetime of the propagating radical during reaction. In conventional radical polymerization, radicals generated by decomposition of the initiator undergo propagation and termination reactions within a second, while the lifetime of the living radical can be extended to several hours in CRP which enables the preparation of polymers with predefined molar masses, narrow polydispersity, controlled compositions and functionality [14]. Metal catalyzed atom transfer radical polymerization (ATRP) is one important CRP method. ATRP has the following features: the polymerization can be performed at very mild conditions (room temperature), with high yield and on a broad range of monomers. The occurrence of transfer reactions (in solution) is negligible, because the radical species are always present at the end of the growing, surface tethered polymer chains [15].

Fig. 1 describes the mechanism of ATRP, where L is a ligand that complexes with the cuprous salt and solubilizes it in the organic reaction system. k_a and k_d are rate constants for activation and deactivation of the halide initiator, with $K = k_a/k_d$. Activation of the initiator involves the CuBr metal center undergoing an electron transfer with simultaneous halogen atom abstraction and expansion of its coordination sphere. R• is the reactive radical that initiates polymerization. $CuBr_2(L)$ is called the deactivator and is the persistent radical that reduces the steady-state concentration of propagating radicals and minimizes normal termination of living polymers [16]. In ATRP, radicals are generated by the redox reaction of alkyl halides (R–Br in Fig. 1) with transition-metal complexes (L in Fig. 1). Radicals can then propagate but are rapidly deactivated by the oxidized form of the transition-metal catalyst ($CuBr_2(L)$ in Fig. 1).

Successful ATRP requires fast initiation (activation of RBr) so that all propagating species begin growth at the same time,

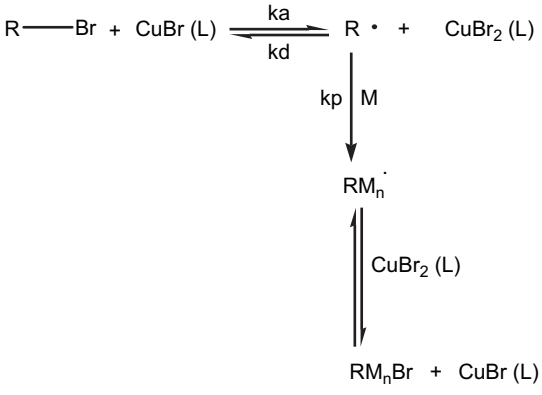

Fig. 1. Schematic mechanism of atom transfer radical polymerization.

which results in a narrow molecular weight distribution. Rapid reversible deactivation of propagating radical is needed to maintain low radical concentrations and minimize normal termination of living polymers. This ensures a narrow molecular weight distribution because all propagating chains grow at the same rate and for the same length of time. The polymer should be approximately monodisperse ($\overline{X}_w \approx \overline{X}_n$) under certain conditions. The polydispersity index (PDI) is given by [17]:

$$\frac{\overline{X}_w}{\overline{X}_n} = 1 + \frac{[I]_0 k_p}{k_d [D]} \left(\frac{2}{p} - 1 \right) \quad (1)$$

where D is the deactivating agent, which is $CuBr_2$ in this system; $[I]_0$ is the concentration of initiator, which is R–Br; P is the fractional conversion of monomer at any time in the reaction; k_p is the rate constant of radical propagation. The molecular weight distribution is narrow with lower initiator concentration, higher conversions, rapid deactivation (higher values of k_d and [D]), and lower k_p values. When these conditions are fulfilled the molecular weight distribution can be simplified as in Eq. (2).

$$\frac{\overline{X}_w}{\overline{X}_n} = 1 + \frac{1}{\overline{X}_n} \quad (2)$$

Eq. (2) shows that the size distribution will be very narrow being close to unity except for a very low molecular weight polymer.

Initiators typically used are α-haloesters (e.g., ethyl 2-bromoisobutyrate and methyl 2-bromopropionate) or benzyl halide (e.g., 1-phenylethyl bromide and benzyl bromide). A wide range of transition-metal complexes such as Ru-, Cu- and Fe-based systems have been successfully applied to ATRP. In Fe-, Cu-based systems, ligands such as 2,2′-bipyridine and aliphatic amines have been employed to tune both solubility and activity of various ATRP catalysts. ATRP has been successfully applied for the controlled polymerization of styrene, methacrylate, methacrylamides, acrylonitrile and 4-vinylpyridine. Muhammad et al. [18] developed the graft polymerization of methyl methacrylate (MMA) by ATRP on an initiator-immobilized substrate. 2-(4-Chlorosulfonylphenyl) ethyl trimethoxysilane was used as an initiator which can be immobilized on oxidized silicon particles. A crosslinked ultrathin polymer film coating on gold was synthesized, using ATRP, by Huang et al. [19] They immobilized the disulfide initiator onto the gold surface followed by surface grafting polymerization by the ATRP approach. Crosslinking is provided by multifunctional ethylene glycol dimethacrylate.

A very stable magnetorheological fluid was synthesized, in which the iron particles are covalently grafted with a poly(butyl acrylate) chain using atom transfer radical polymerization. In this reaction system, an ATRP initiator, 2-(4-chlorosulfonylphenyl)-ethyltrichlorosilane (CTCS), is immobilized on the iron particle surface which then initiates radical polymerization. Then the polymers are grafted from the surface of iron particles [20]. Fig. 2 shows a schematic of the surface-initiated ATRP approach. The sedimentation behavior of iron particles is well known. After the particles are surface treated with ATRP the settling rate is significantly reduced. The effect of ATRP on rheological properties, such as shear, yield stress and viscosity, was also investigated.

2. Experimental and instrumentation

2.1. Materials

The MR fluid with the particles treated by ATRP includes carbonyl iron particles, carrier fluid, and polymer. Carbonyl iron particles (ISP Technologies Inc., Grade-R-2430) are 99.7% pure iron and are formed by thermal decomposition of iron pentacarbonyl $Fe(CO)_5$. The average diameter of the ferrous particles is about 3–4 μm. Fig. 3 is a scanning electron microscopic image of carbonyl iron particles. Each MR fluid sample contains 81 wt% carbonyl iron particles. The carrier fluid is an organic polar solvent typically chosen based on its viscosity, freezing and boiling points and vapor pressure. The solvent used is *N*-octyl-pyrrolidone (Aldrich Chemical

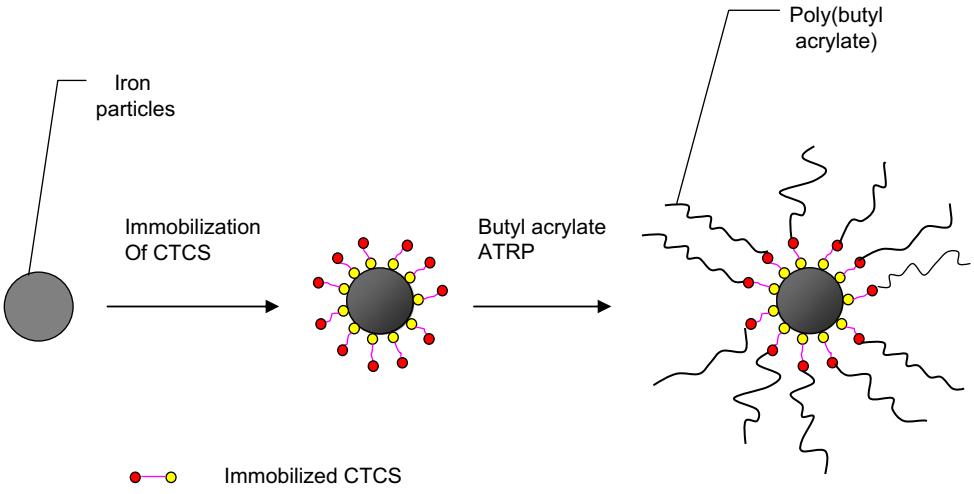

Fig. 2. Schematic of ATRP approach for surface-initiated polymerization on iron particles.

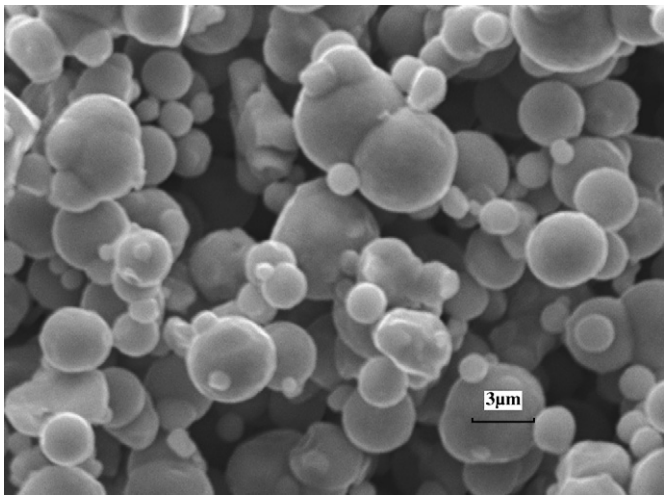

Fig. 3. Scanning electron microscopic image of pure iron particles.

Company, Inc.), which has a boiling point of 306 °C, viscosity of 9 cp at 20 °C and a vapor pressure of less than 1.3 Pa at 20 °C. Butyl acrylate, copper bromide (CuBr, 99%), and L-(−)-sparteine (Sp) were obtained from Aldrich. Initiator 2-(4-chlorosulfonylphenyl)-ethyltrichlorosilane (CTCS), which dissolved in 50 wt% toluene, was purchased from Gelest. All the reagents are used as received without further purification.

2.2. Immobilization of initiator and graft polymerization

Iron particles, 290 g, with an average diameter of 3–5 μm were dried in vacuum at 40 °C for 24 h. The dried particles were then dispersed in 100 g of non-polar solvent, toluene. CTCS with a chlorosulfonylphenyl group, which is an excellent initiating group for ATRP, was immobilized on the surface of iron particles by the self-assembled monolayer-deposition method [20]. CTCS, 0.1 g, in 100 g toluene was dripped into the iron particle, toluene suspension. The mixture reacted at room temperature and was kept in vacuum for 24 h. The theoretically calculated initiators attached on the iron particle surface are about 3.5 nm^2. The particles treated with initiator were then washed with tetrahydrofuran (THF) several times and dried in vacuum at room temperature for 24 h [21,22].

The CTCS-functionalized iron particles were grafted with poly(butyl acrylate) using the ATRP approach. A degassed *N*-octyl-pyrrolidone (62 g) solution containing 6.9 g butyl acrylate, 0.04 g CuBr, 0.06 g Sp, 0.02 g $CuBr_2$, and 290 g initiator coated iron particles was sealed in a reactor. The mixture was reacted in vacuum at 70 °C for 8 h. Sp is the ligand coordinating with CuBr, providing a homogeneous ATRP system for butyl acrylate. After polymerization, the resultant suspension is the magnetorheological fluid system.

2.3. SEM and FTIR

Various techniques were used to highlight the surface modification of iron particles. IR spectra were carried out in a Fourier transform infrared (FTIR) spectrophotometer at room temperature, using the KBR pellet method. Scanning electron microscopy (SEM) was used to characterize the surface of both pure iron particles and surface-initiated ATRP treated particles.

2.4. Magnetorheological rheometer

The instrument used to measure rheology is Anton Paar Physica MER300, operating in either stress or strain controllable mode. A detail description of this technique has been given in other literature [23]. This instrument was used to measure the off-state apparent viscosity and shear yield stress of MR fluids under controlled magnetic fields.

2.5. Particle settling

Sedimentation of iron particles by gravity causes severe problems with the operation of devices utilizing magnetic fluids. Sedimentation is a direct consequence of the greater density of iron particles than that of the carrier medium. When the particles' size is sufficiently small (<1 μm), the gravitational force is opposed by a diffusion force associated with thermal Brownian motion. However, the yield stress of MR fluid decreases when reducing the size of the iron particles. We used surface-initiated ATRP to modify the surface of iron particles, to improve the stability and the durability of MR fluid.

Two different methods are used to describe the settling behavior of MR fluids. One method is the measurement of the sedimentation behavior of particles in a carrier medium through visual observation [24]. This method is done by measuring the formation of a clear fluid layer on the surface of the MR fluid when a sample is permitted to settle for a period of time at room temperature. This layer is measured as the clear fluid volume fraction when the iron particles settle into the carrier fluid in a graduated glass cylinder. The change of clear fluid volume is measured as a function of time. The advantage of the method is its simplicity. However, this method cannot be applied in opaque media and much time is needed for a slowly sedimenting suspension.

Another method to measure the settling behavior is described by Gorodkin et al. [25]. The settling velocity of iron particles is characterized by a sedimentation constant parameter. Sedimentation of the iron particles causes the upper layer of MR fluid to have a lower concentration of iron particles and therefore lower permeability. The MR fluid fills the tube such that the particles are at the top of the solenoid windings and rotor rotation supplies a centrifugal force promoting sedimentation of the iron particles. These particles travel a distance x, leaving less material within the solenoid. This sedimentation leads to a reduced inductance in the solenoids. The rate of change of the magnetic permeability of the MR fluid in the upper layer can be used as a measure of the sedimentation velocity of the particles. Sedimentation rate of the iron particles in MR fluid is estimated with the sedimentation constant

S, which is the ratio of a sedimentation velocity u to the acceleration of gravity g.

$$S = u/g \tag{3}$$

where Svedberg (1 Sb = 10^{-13} s) is taken as a unit of measurement of S. As described in Ref. [25], the sedimentation constant S defined in Eq. (1) is given by:

$$S = \frac{900 \ln(1 + x/R_0)}{\pi^2 n^2 t} \tag{4}$$

where x is the distance traveled by particles for a time t, R_0 is the initial radius of the particles relative to the rotation center, n is the rotation rate of the centrifuge shaft in rpm. The distance traveled by particles x is given by:

$$x = l\frac{L_{max} - L}{L_{max} - L_0} \tag{5}$$

where l is the length of solenoid, L_{max} is the solenoid inductance before the onset of sedimentation, L_0 is the inductance of vacuum and L is the inductance at time t.

2.6. Step-scan DSC

Step-scan DSC is performed on a Perkin Elmer Pyris 1 DSC, using the built in software provided. Step-scan DSC is used for the characterization of the thermal properties of materials, including glass transition temperature T_g. The step-scan DSC is used to separate reversible from irreversible phenomenon. With the application of heating over small temperature increments, and by holding for a short time interval, the heat capacity, Cp, reflects the reversible aspects of the sample. Kinetic or irreversible effects are eliminated in the thermodynamic Cp data. For example, if a sample has a glass transition, T_g, which has overlapping moisture loss or crystallization event, the thermodynamic Cp signal will show the classic stepwise change in the heat capacity, which makes it simple and straightforward to analyze and interpret. The step-scan DSC approach also provides the kinetic or IsoK baseline data set, which is reflective of the irreversible or slow processes taking place during the experiment. The enthalpic relaxation, moisture or crystallization event will show up in the IsoK baseline data. In the case of polymers with residual solvent, step-scan DSC is an effective means for measurement of the glass transition temperature (T_g) because it allows separation of the thermal transition due to the T_g from evaporation of the solvent. Heat rate is 5 °C/min for the temperature range of −64 to 29 °C. Isothermal hold time is 0.5 min/cycle and 55 cycles are performed. Helium is used as purge gas at 20 ml/min. The data subsequently are analyzed to determine the reversing and non-reversing components.

3. Results and discussion

3.1. Initiator immobilization and ATRP of butyl acrylate on iron particles

The self-assembled monolayer-deposition method to prepare iron particles carrying chlorosulfonylphenyl groups suitable for atom transfer radical polymerization is used to synthesize MR fluids. Fig. 4 illustrates the process used to immobilize initiator on the iron particles' surface. It shows that chlorosilyl groups of CTCS react with hydroxyl groups on the surface of iron particles to yield a covalent bond Si–O–Fe, thus forming a monolayer of initiator on the surface. The formation of initiator monolayer on iron particles' surface is confirmed by the FTIR spectrum. Fig. 5 shows the FTIR spectra of pure iron particles (curve a) and iron particles treated by CTCS (IP-CTCS curve b). The spectrum of IP-CTCS has an absorption peak at 1371 cm^{-1}, which corresponds to the covalent bond S=O stretching of CTCS. The other characteristic band at 1171 cm^{-1} is due to the Si–O stretch.

A fundamental concept of ATRP is the halogen exchange in the polymerizing system between the halogen-terminated growing polymer chain/Cu(I)Br complex and macroradical/Cu(II) complex. Radicals are created by the redox reaction between CTCS and CuBr/sparteine complex. In this reaction, Cu(I) is oxidized to Cu(II) by losing an electron while chloride atom in CTCS is reduced to Cl^{-1} by obtaining the electron from Cu(I). In this way, a free radical is produced, which is shown in Fig. 6. In this free radical producing process, all the initiators decompose at once or in a very short time period so that all propagating radicals grow for very close to the same time.

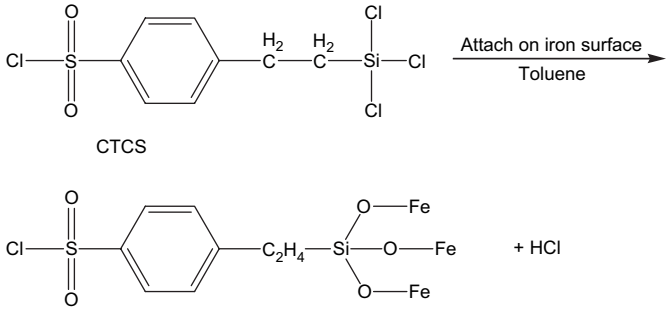

Fig. 4. Initiator attaches on iron particles' surface.

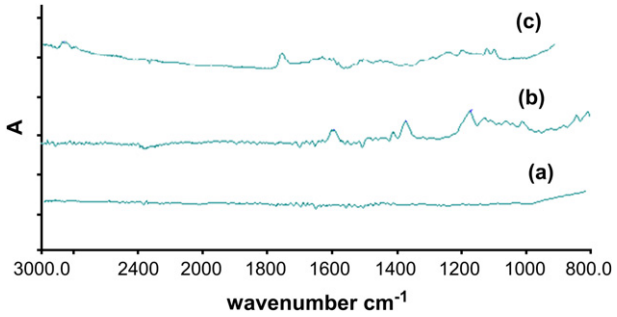

Fig. 5. FTIR spectra of (a) pure iron particles, (b) iron particles coated with initiator layer and (c) iron particles treated with ATRP poly(butyl acrylate).

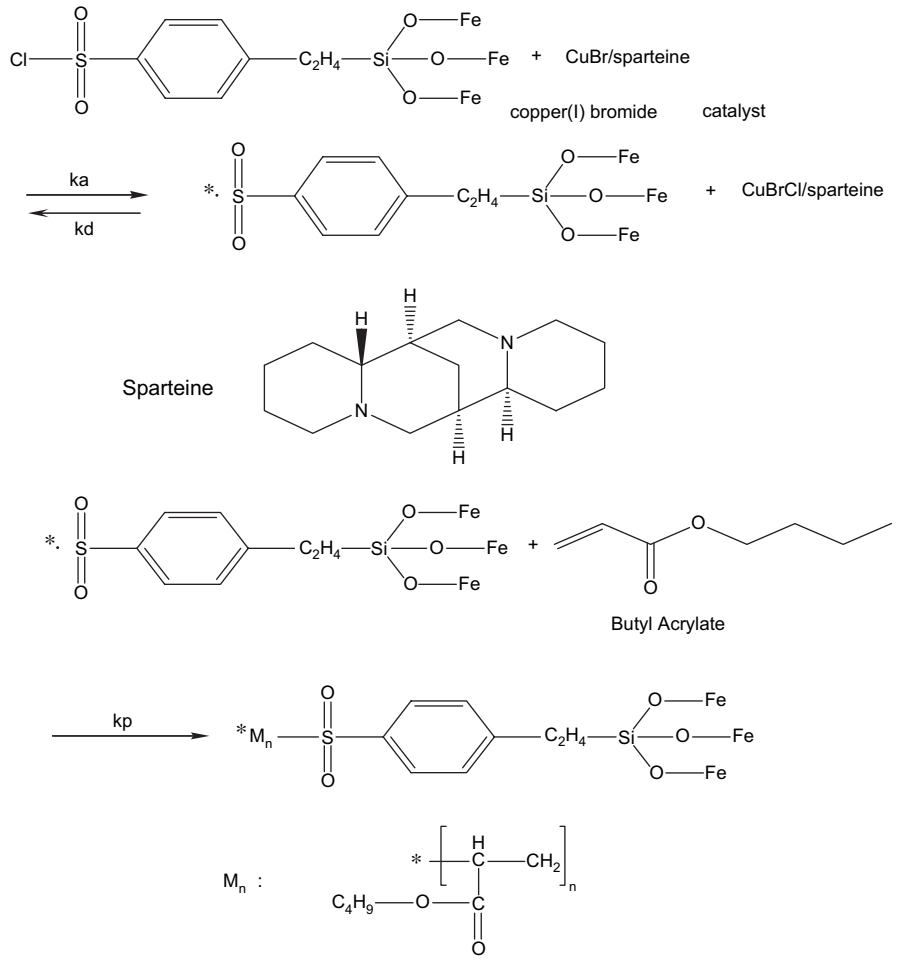

Fig. 6. Free radical formation by redox reaction and chain propagation in ATRP process.

Fast initiation is important, however, it is the fast equilibrium between the propagating radical and dormant species with an appropriate equilibrium constant K that determines the living characteristics of these reaction systems [26]. The reactive radicals quickly initiate polymerization of butyl acrylate (shown in Fig. 6). The equilibrium constant must be low but not too low; that is, the concentration of propagating radical must be sufficient to achieve a reasonable propagation rate but not so high that normal bimolecular termination becomes predominant.

Cu(II) salt acts as a controlling or mediating agent because it is sufficiently reactive to couple rapidly with propagating chains to convert them reversibly into dormant, nonpropagating species. The overall result is that, with the introduction of the dormant state for living polymers, the bimolecular termination of living polymer is suppressed, and the average lifetime for living polymers is increased by at least four orders of magnitude. Fig. 7 shows the schematic of equilibrium between dormant polymer chain and propagating macroradical. Better

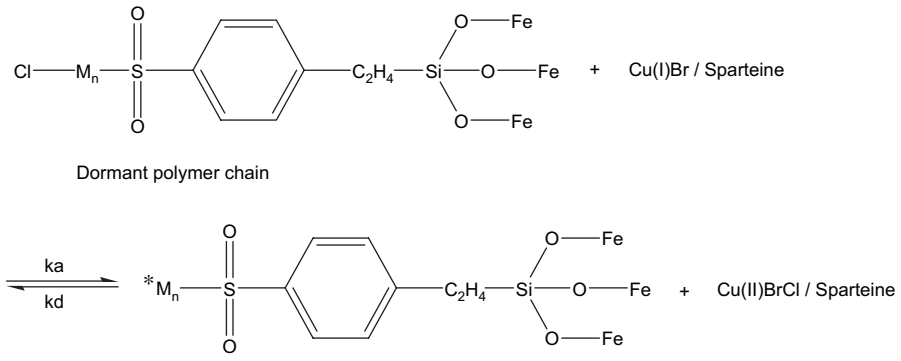

Fig. 7. Schematic of equilibrium between dormant species and propagating radical.

control over surface-initiated polymerization can be achieved by the addition of Cu(II)Br_2 to the monomer solution [27].

The accomplishment of surface-initiated ATRP on iron particle surfaces is confirmed through FTIR analysis shown in Fig. 5. Compared to the pure iron particles (curve a), there is an intense absorption peak at 1732 cm^{-1}(curve c) due to the C═O stretching of the carbonyl group of poly(butyl acrylate) in the spectrum of iron particles whose surfaces were treated with surface-initiated ATRP process. The observed poly(butyl acrylate) was grown from the surface of the iron particles because the polymerization could initiate only from the surface-bound CTCS and the treated iron particles were washed with THF followed by evaporation in the vacuum oven. The other characteristic absorption band at 2955 cm^{-1} is due to the C–H stretch in poly(butyl acrylate).

SEM experiments revealed particles' morphology before and after the ATRP reaction. Fig. 8 shows the SEM images of pure iron particles and ATRP treated iron particles. After surface-initiated ATRP reaction the surface of the particles becomes slightly rougher and some interparticle bridging appears.

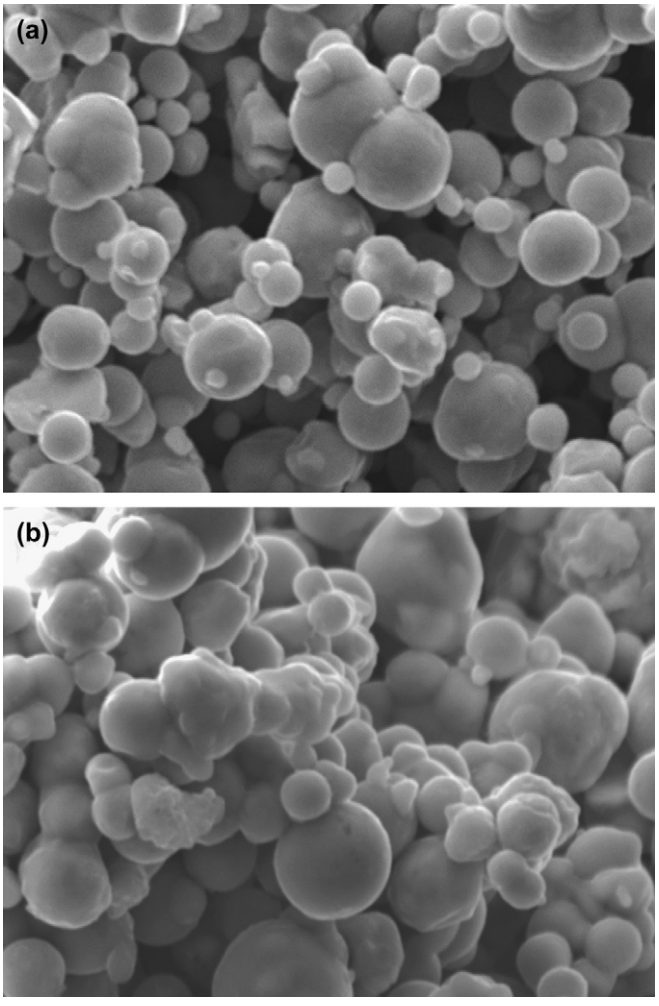

Fig. 8. SEM images of pure iron particles (a) and ATRP treated iron particles (b).

3.2. Polymerization analysis of bulk butyl acrylate ATRP

ATRP proceeds via the establishment of a dynamic equilibrium between the active and dormant species as shown in Fig. 1. The overall rate of polymerization and the level of control during the polymerization are influenced by several internal variables, such as initiator catalyst, ligand, type of transferring halogen (X), and external variables such as temperature and time [28]. The polymerization of bulk butyl acrylate is carried out in a sealed tube by using CuBr as catalyst and sparteine as ligand in the presence of initiator CTCS at certain temperature, time and concentration of butyl acrylate. The synthesized poly(butyl acrylate)s are precipitated in methanol and filtered. The polymers are dried in a vacuum oven. The conversion is calculated from the weight of dried polymer to that of monomer. The molecular weight of polymer is calculated using Mark Houwink parameters for the homopolymers found by testing three standard polymers whose molecular weights are known. Intrinsic viscosities are measured using a Cannon Ubbelohde viscometer (size 50) at 22 °C using toluene as solvent.

During polymerization, the relation between molecular weight and conversion with the molar ratio of butyl acrylate is shown in Table 1. Polymerization is carried out at conditions: [CTCS]:[CuBr]:[Sparteine] = 1:1:1, at 70 °C. As shown in Table 1, the molecular weight increases with an increase of the molar ratio of butyl acrylate to initiator. For example, the molecular weight of polymer synthesized with molar ratio of CTCS to butyl acrylate at 1:500 is nearly seven times than that at 1:100. It is believed that the molecular weight of coating polymer can affect the viscosity and settling rate of MR fluid. For example, if the molecular weight is too small, the coating polymer cannot prevent iron particles from settling, whereas, if it is too large, the viscosity of off-state MR fluid will be high. Therefore, the molar ratio 200:1 between monomer and initiator is used in this synthesis.

Polymerization of butyl acrylate was carried out at 70 °C using [CTCS]:[CuBr]:[Sparteine] = 1:1:1 for different times. The results are summarized in Table 2. The radical polymerization rate can be expressed in the following equation [16]:

$$-\mathrm{d}[\mathrm{m}]/\mathrm{d}t = k_\mathrm{p}[\mathrm{p}^\bullet][\mathrm{M}] \tag{6}$$

By integration of Eq. (6), the kinetic equation can be obtained as:

$$\ln[\mathrm{M}]_0/[\mathrm{M}] = k_\mathrm{p}[\mathrm{p}^\bullet]t = k_\mathrm{p}^{\mathrm{app}}t \tag{7}$$

Table 1
ATRP of butyl acrylate initiated by CTCS under various ratios of butyl acrylate to initiator in bulk

Butyl acrylate	Initiator (CTCS)	Reaction time (min)	Conversion (%)	MW (experimental)	MW[a] (calc)
100	1	480	54	5100	6912
200	1	480	59	13 800	15 104
300	1	480	62	22 000	23 808
400	1	480	63	33 200	32 256
500	1	480	58	35 800	37 120

[a] The calculated molecular weight is equal to the sum of molecular weight of initiator and $[\text{butyl acrylate}]_0/[\text{CTCS}]_0 \times \text{conversion} \times 128$.

Table 2
Polymerization of butyl acrylate at 70 °C at different time scales, where [CTCS]:[CuBr]:[Sparteine] = 1:1:1

Butyl acrylate	Initiator (CTCS)	Reaction time (min)	Conversion (%)	$\ln[M]_0/[M]$	MW (experimental)	MW (calc)
200	1	60	12	0.128	4300	3072
200	1	120	19	0.210	6450	4864
200	1	240	38	0.478	12 000	9728
200	1	360	50	0.693	12 900	12 800
200	1	480	59	0.890	13 800	15 104

From Eq. (7), we can obtain k_p^{app} from the plot of $\ln[M]_0/[M]$ vs time. The molecular weight of poly(butyl acrylate) determined from viscometry agrees well with the calculated molecular weight.

Fig. 9 shows the variation of conversion and $\ln[M]_0/[M]$ with time at 70 °C. The conversion increases with time. An auto-acceleration phenomenon is observed at the early state reaction. Fig. 9 also reveals a semi-logarithmic behavior of this reaction. The plot is close to linear indicating the number of active species that remains constant throughout the reaction, which reveals that $k_p[p^{\bullet}]$is constant, and the molecular weight of polymer can be controlled by the initial molar ratio of the monomer and initiator, and conversion. All of these results indicate that the ATRP of butyl acrylate in bulk is first order with respect to monomer concentration at reaction temperature of 70 °C.

The molecular weight as a function of reaction temperature is shown in Fig. 10. Again, the polymerization condition is that [butyl acrylate]:[CTCS]:[CuBr]:[Sparteine] = 200:1:1:1 with the reaction time of 480 min. It can be seen that MW of poly(butyl acrylate) increases on increasing the reaction temperature from 50 to 90 °C and decreases with further increase in reaction temperature to 100 °C. This can be attributed to the fact that the rate of chain propagation increases with reaction temperature. However, the rate of chain transfer also increases with temperature. The molecular weight decrease at higher temperature is therefore attributed to the increased rate of chain transfer compared to chain propagation [29].

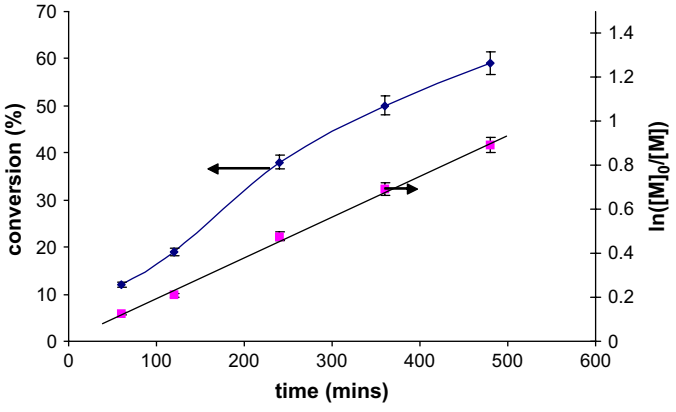

Fig. 9. Conversion and $\ln[M]_0/[M]$ against polymerization time for bulk ATRP of butyl acrylate at 70 °C; [butyl acrylate]:[CTCS] = 200:1.

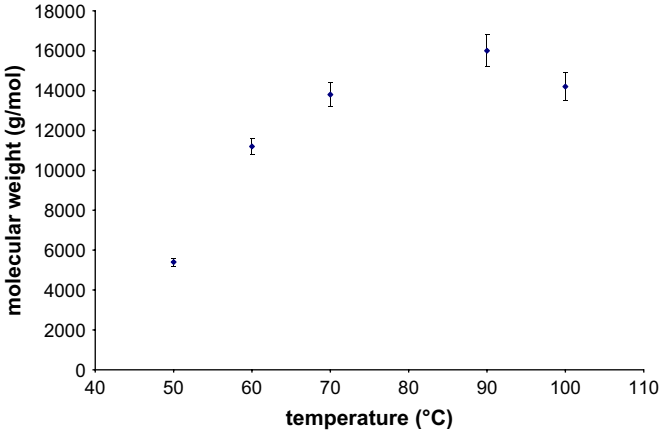

Fig. 10. Variation of molecular weight with polymerization temperature.

3.3. Glass transition temperature measured by step-scan DSC

The glass transition temperature (T_g) of the synthesized ATRP poly(butyl acrylate) is measured using step-scan DSC. Two parameters are measured, one is the thermodynamic Cp, which reflects the reversible behavior of the material, and the other is the IsoK baseline representing the irreversible or kinetic behavior. The following equation describes the total heat flow:

$$dH/dt = Cp(dT/dt) + f(T,t) \quad (8)$$

Cp is the sample heat capacity, dT/dt is the heating rate, and $f(T,t)$ is irreversible or kinetic component of the heat flow and is a function of time and temperature. Therefore, the heat capacity on heating is related to the change in heat flow divided by the change in temperature and the non-reversing heat flow is the change in heat flow that occurs during the isothermal segment of the heat-hold experiment [30]. Reported advantages of SSDSC over conventional DSC include improved sensitivity and resolution, separation of overlapping reversing and non-reversing transitions and more accurate heat capacity values [31]. Irreversible processes include enthalpic relaxation and solvent or moisture evolution. When the sample is maintained at constant temperature the heating rate, dT/dt, is 0 °C/min and the heat flow is due to kinetic behavior. Step-scan DSC separates out the reversible transition (T_g) and the kinetic events thus providing a clear identification of the T_g of the material from the Cp curve. Fig. 11 shows that the glass transition temperature of poly(butyl acrylate) is about −47 °C, which is close to the literature value [32].

3.4. Shear yield stress

Fig. 15 shows shear stress behavior of the MR fluid. These data demonstrate Bingham fluid type behavior. The Bingham behavior can be expressed as follows:

$$\tau = \boldsymbol{\tau}_y + \eta\dot{\gamma}, \quad \tau \geq \tau_y \quad (9)$$

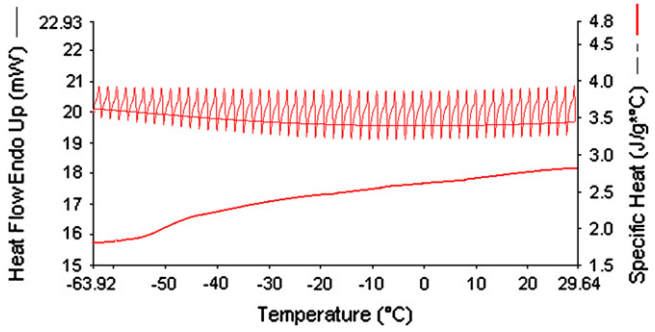

Fig. 11. Step-scan DSC results on ATRP poly(butyl acrylate).

where τ is the total shear stress, τ_y is the field-controllable shear yield stress, η is the plastic viscosity, and γ is the shear rate. Using the Bingham model, the dynamic yield stress τ_y is determined for each curve by extrapolating the shear stress to zero shear rate and finding the intersection with the vertical axis. For example, from Fig. 12, the yield stress of MR fluid is about 3.0×10^4 Pa at 0.529 T.

As expected, the shear stress increases with increasing magnetic flux density. To examine the field dependence of the stress, a log–log plot of the stress vs magnetic flux density B is obtained under four different shear rates, as shown in Fig. 13. The slope of the shear stress vs magnetic fluid density is 1.47. Therefore, the field dependence of the shear stress is given by $B^{1.47}$, which is close to the theoretical prediction of $B^{1.5}$ calculated by Ginder and coworkers [33].

Direct microscopic observation of MR fluid reveals that the microstructure consists of chains or columns of particles aligned in the direction of the magnetic field, because the induced dipoles cause the particles to align "head to tail" in chains and parallel to the applied field. Under low shear rates these chains or columns are sheared, eventually rupturing at some critical strain (the stress at this critical strain is called yield stress) and then reforming with other ruptured chains which are carried past by the shear flow.

The effect of weight ratio of polymer to iron particles on shear stress is investigated. Experiments show that the increase

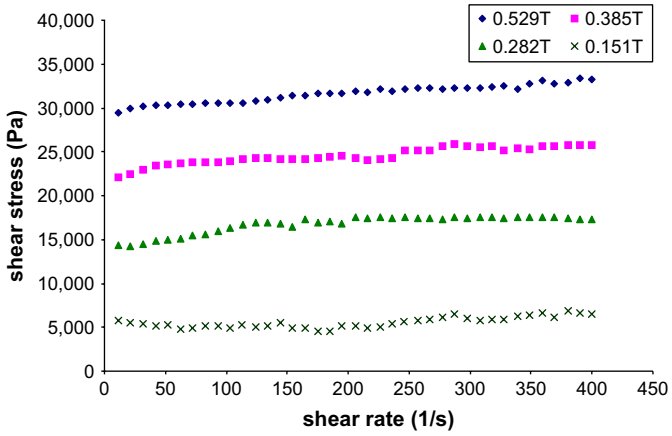

Fig. 12. Flow curves for the ATRP magnetorheological fluid under different magnetic flux densities.

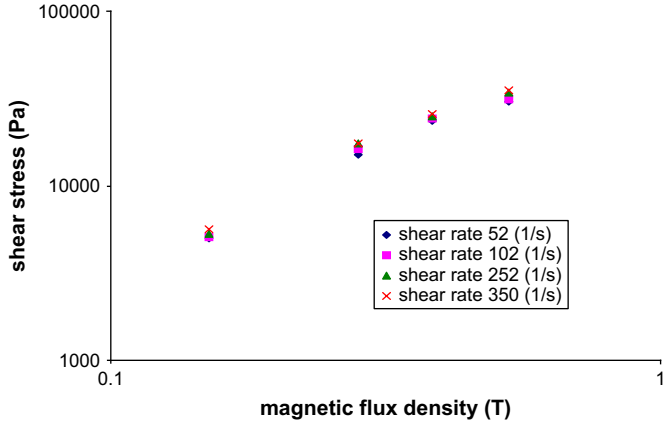

Fig. 13. Log–log plot of shear stress vs magnetic fluid density B under different shear rates.

in weight of poly(butyl acrylate) decreases the shear stress. This is because when the thickness of the coating polymer increases the local saturation of the magnetic particles will be reduced as well as the yield stress of the MR fluid, as shown in Eq. (10) [33]:

$$\tau_y \propto \phi \mu_0 M_s^{1/2} B^{3/2} \tag{10}$$

where $\mu_0 = 4\pi \times 10^{-7}$ T m/A is the permeability in free space, ϕ is the volume fraction of carbonyl iron particles, M_s is the local saturation of magnetization and B is the magnetic induction related to the external field H_0 by the following equation:

$$B = \mu_0(H_0 + M_s) \tag{11}$$

A commercially available MR fluid is tested as a benchmark to compare with the MR fluid treated with ATRP. The shear stresses for both of these MR fluids are nearly identical.

3.5. Viscosity of ATRP MR fluid

The apparent viscosity is defined as the slope of shear stress/shear rate curve. An important feature of ATRP MR fluids is that the off-state viscosity can be controlled by the concentration of poly(butyl acrylate). Fig. 14 shows the off-state viscosity at room temperature. The shear stress increases with an increase in the concentration of polymer coating on the surface of the iron particles, as shown in Fig. 14. For example, at 0.5%, 1.5% and 2% concentrations polymer can yield the increasing off-state viscosities of 0.13, 0.16 and 0.18 Pa s, respectively. The shear stress data show shear thinning behavior. Low viscosity MR fluids are desirable for certain applications, including dampers.

3.6. Particles' settling

A criterion for achieving good particulate dispersion is to ensure that the polymer coats the particle surface homogeneously. If the particle coating is complete, settling, which is due to gravitational forces, is reduced. The stability of

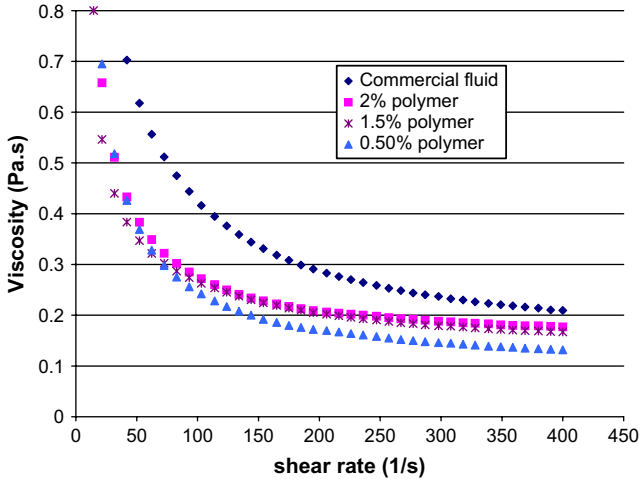

Fig. 14. Off-state viscosity of ATRP MR fluid.

magnetorheological (MR) suspensions has been investigated by Rankin et al. using the gravity yield parameter, Y_G [34].

$$Y_G = \tau_0^G / [gR(\rho_p - \rho)] \quad (12)$$

where τ_0^G is the yield stress of the carrier medium, g is the acceleration of gravity, R is the particle radius, ρ_p is the iron particle density, and ρ is the density of the carrier medium. Larger values of Y_G indicate better stability of the MR suspension. If Y_G is greater than a critical value, $Y_{Gcritical}$, (for each particulate material a critical viscoplastic yield stress can be defined) the carrier medium will prevent a particle from settling. But for medium having larger values of Y_G, very high off-state viscosity results so the MR suspension response time to the magnetic field increases and MR fluid applications are limited.

Fig. 15 shows the settling behavior of commercial MR fluid, and ATRP MR fluid with different poly(butyl acrylate) concentrations of coating on the iron particles. All the samples have 81% iron particles. The settling curve depends on the concentration of polymer coating on iron particles. Particle settling is reduced by increasing the coated polymer fraction. However, we know that the shear yield stress will be reduced

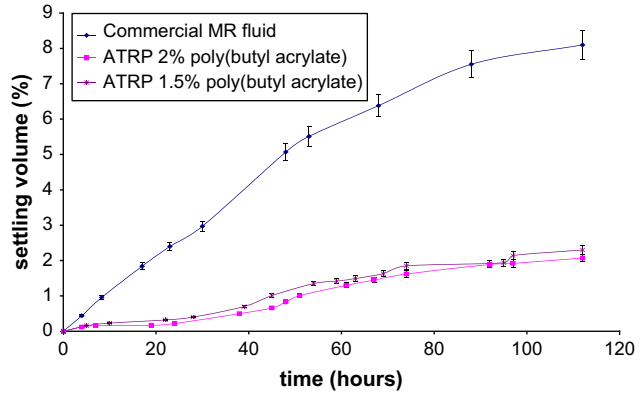

Fig. 15. Settling curves of various ATRP MR fluids and commercial MR fluid.

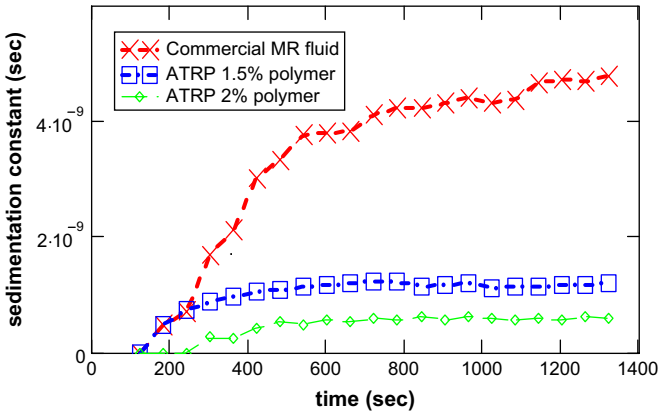

Fig. 16. Settling rate of ATRP MR fluids and commercial MR fluid.

when increasing the amount of polymer coating on the surface of iron particles. Poly(butyl acrylate) at 1.5% is used for coating the iron particle surface. The sedimentation is 7.5% at 110 h for commercial MR fluid while it is only about 1.5 wt% for ATRP MR fluid with 1.5 wt% polymer on the particles. The settling behavior of MR fluid only containing pure iron particles and carrier fluid, and ATRP MR fluids is also tested. The untreated iron particles precipitate quickly in a short time, while iron particles treated with ATRP method are well dispersed and no significant settling behavior is observed. Thus, grafting poly(butyl acrylate) on iron particles has significantly improved dispersibility. The explanation for this behavior is the formation of ATRP layer, which exists on the surface of the iron particles and acts as a stabilizing layer to sterically prevent coagulation.

Fig. 16 shows the settling velocity curves for commercial MR fluid, and ATRP MR fluids by measuring the sedimentation constant. This result is consistent with the measurement shown in Fig. 15. ATRP MR fluids have lower settling rate than commercial MR fluid. The curves in Fig. 16 correspond to the slope of the corresponding curves in Fig. 15 because the curves in Fig. 15 describe the change of position of iron particles with time, so that the slopes of these curves indicate the settling velocity of iron particles while average velocity of settling is exhibited in Fig. 16.

4. Conclusion

Surface-initiated atom transfer radical polymerization (ATRP) was used to treat the surface of iron particles to stabilize the dispersion. The process includes two steps: immobilization of initiator CTCS onto iron particles' surface, and atom transfer radical polymerization of poly(butyl acrylate). FTIR and SEM were used to characterize the surface of treated and untreated iron particles to confirm the formation of the polymer layer coating on particles surface. The polymerization analysis of ATRP of butyl acrylate was investigated. It was found that the molecular weight and conversion are controlled by the temperature, time, and concentration between monomer and initiator. The glass transition temperature of ATRP poly(butyl acrylate) is −47 °C. The rheological properties of MR

fluid synthesized by ATRP were investigated using a magnetic rheometer. Experiments confirmed that the rheological behavior can be described by the Bingham equation. Similar to a magnetorheological polymer gel, the off-state viscosity of ATRP MR fluid can also be controlled by the amount of polymer in the system. The stability of the MR fluid was greatly improved by surface polymerization using ATRP.

References

[1] Ginder JM. In: Encyclopedia of applied physics, vol. 16; 1996. p. 487.
[2] David Carlson J, Jolly Mark R. Mechatronics 2000;10:555.
[3] Klingenberg Daniel J. AIChE J February 2001;47:246.
[4] Wilson M, Fuchs A, Gordaninejad F. J Appl Polym Sci 2002;84:2733.
[5] Fuchs A, Gordaninejad F, Blattman D, Hamann G. U.S. pat. 6,527,972; 2003.
[6] Fuchs A, Mei X, Gordaninejad F, Xiaojie W, Gregory HH, Gecol H, et al. J Appl Polym Sci 2004;92:1176.
[7] Yammoto M, Ohata M. Prog Org Coat 1996;27:277.
[8] Ma M, Zhang Y, Yu W, Shen HY, Zhang HQ, Gu N. Colloids Surf A Physicochem Eng Asp 2003;212:219.
[9] Marcus W, Jackiw Jennifer J, Rossi RR, Weiss PS, Grubbs RH. J Am Chem Soc 1999;121:4088.
[10] Namyong YK, Jeo NL, Choi IS, Takami S, Harada Y, Finnie Krista R, et al. Macromolecules 2000;33:2793.
[11] Xing YF, O'Shea SJ, Li SFY. J Electroanal Chem 2003;542:7.
[12] Huang XH, Huang HZ, Wu NZ, Hu RS, Zhu T, Liu ZF. Surf Sci 2000;459:183.
[13] Eizo M, Shinpei Y, Tsedev N, Yoshinobu T, Takeshi F, Mikio T. Polymer 2004;45:2231.
[14] Pyun J, Matyjaszewski K. Chem Mater 2001;13:3436.
[15] Bontempo D, Tirelli N, Feldman K, Masci G, Crescenzi V, Hubbell JA. Adv Mater 2002;14:1239.
[16] Odian G. Principles of polymerization. John Wiley & Sons, Inc; 1991 [chapter 3].
[17] Kowalewski T, Mccullough RD, Matyjaszewski K. Eur Phys J E 2003; 10:1.
[18] Muhammad E, Shinpei Y, Kohji O, Yoshinoby T, Takeshi F. Macromolecules 1998;31:5934.
[19] Huang WX, Baker GL, Bruening ML. Angew Chem Int Ed 2001; 40:1510.
[20] Marutani E, Shinpei Y, Tsedev N, Yoshinobu T, Takeshi F, Mikio T. Polymer 2004;45:2231.
[21] Ejaz M, Yoshinoby T, Takeshi F. Polymer 2001;42:6811.
[22] Tesedev N, Shinpei Y, Takeshi F. Solid State Sci 2004;6:879.
[23] Li WH. Rheology of MR fluid and MR damper dynamic response: experimental and modeling approaches, PhD dissertation, NanYang Technological University; 2000.
[24] Fuchs A, Xin M, Gordaninejad F, Wang XJ, Gregory HH, Gecol H, et al. J Appl Polym Sci 2004;92:1176.
[25] Gorodkin SR, Kordonski WI, Shorey AB, Jacobs SD. Rev Sci Instrum 2000;71(6):2476.
[26] Odian George. Principles of polymerization. John Wiley & Sons, Inc; 2004 [chapter 3].
[27] Kim JB, Huang WX, Miller MD, Baker GL, Bruening ML. J Polym Sci A1 2003;41:386.
[28] Sreepadaraj K, Han G, Bert K, Piet L. Macromolecules 2003;36:8304.
[29] Jiang G, Wang L, Chen T, Yu HJ. Polymer 2005;46:81.
[30] Sandor M, Bailey NA. Polymer 2002;43:279.
[31] Gunaratne LMWK, Shanks RA. Acta 2005;430:183.
[32] Garcia-Domenech R, Julian-Ortiz JV. J Phys Chem B 2002;106: 1501.
[33] Ginder JM, Davis LC, Elle LD. Int J Mod Phys B 1996;10:3293.
[34] Rankin PJ, Hovath AT, Klingenberg DJ. Rheol Acta 1999;38:471.